The galaxy UV luminosity function at z≈2-4: new results on the faint end slope and its evolution

Shegy Parsa
shp@roe.ac.uk
Supervisors : Jim Dunlop, Ross McLure

Introduction

The UV luminosity function (LF) is a fundamental tracer of galaxy formation and evolution. Observations suggest that the star formation rate and AGN activity peak at 2<z<4 which makes this epoch an important era to be studied. Several techniques are available to select galaxies at intermediate redshifts; color selection strategies such as LBG/BM/BX that are based on the rest-frame UV photometry or a reliable photometric redshift catalogue to select sources at a given redshift range.

In this study we use the combination of extremely deep near-IR imaging of the HUDF with the wider CANDELS/GOODS-S H_{160}-band photometric catalogues enabling us to measure the rest-frame UV luminosity function down to very faint magnitudes.

Method

In this work the galaxy sample within redshift range $1.5 < z_{phot} < 4.5$ is selected based on our derived multi-wavelength UV +optical+near-Infrared photometric redshift catalogues of the HUDF12 and the GOODS-S generated using Le Phare (Ilbert et al. 2006). The redshift distribution of our sample is shown in Figure 1.

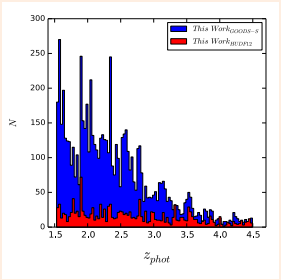

Figure 1. The redshift distribution of our sample (8453 objects in total). The red histogram shows the HUDF12 objects and the blue histogram shows objects selected from the GOODS-S.

Discussion and Implications

z≈2

The main measured z≈2 UV LF at 1500Å is shown in the top panel of Figure 2 along with the recent determinations by Weisz et al. (2014), Alavi et al. (2014) and Oesch et al. (2010). Our use of the latest deep HST imaging has enabled us to extend our measurement of the UV LF down to M_{1500}= -14.5 reaching ~3.5 magnitude fainter than previous determinations.

Our calculated Schechter parameters are M*=-19.83±0.09, ϕ*=6.50±0.75(10^{-3} $Mpc^{-3}mag^{-1}$) and α=-1.34±0.03. As shown in Figure 2, the LF measured by Alavi et al. (2014) and Oesch et al. (2010) via the UV-dropout technique suggest a much steeper faint-end slope of α≈-1.74 and -1.60 respectively.

The lower panel of Figure 2 shows the fitted value of the faint end slope, α, down to each magnitude bin and indicates that this parameter stabilizes at α≈-1.34 over the faintest bins. This result is in a good agreement with the value determined for the faint end slope via the galactic archaeology techniques (e.g. Weisz et al. 2014).

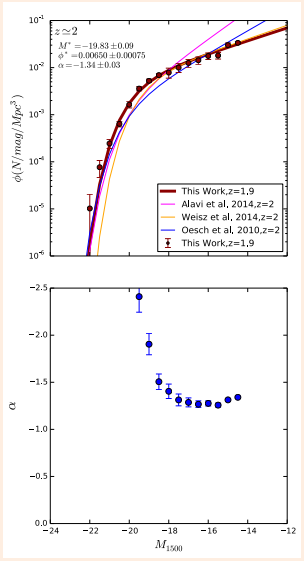

Figure 2. Our measured UV LF at z≈2 with the best-fitting Schechter function. The top panel shows our results along with those of several recent studies for comparison. The lower panel shows the measured faint-end slope down to each magnitude bin confirming the accuracy of our shallower determined α at z≈2.

z≈2-4

Figure 3 shows our determined UV LF for z≈2-4. Our analysis suggests little evolution in α but a significant drop in ϕ* (by a factor of ~2) between z≈2 to z≈4 and brightening in M* (by ~1 mag) over the same redshift range. This evolving trend of M* is consistent with previous studies although the decrease in ϕ*, with increasing redshift is the opposite of some suggestions in the literature. Our determined LFs along with some previous studies are shown in Figure 4.

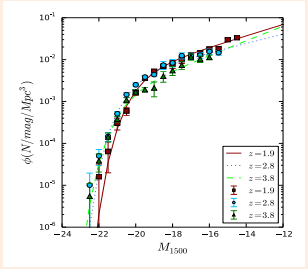

Figure 3. Evolution of the UV LF at z≈2-4. There is little evolution between z≈2 to 3 but a significant drop in ϕ* from z≈3 to 4.

Comparison to Previous Studies

Figure 5 shows our measured Schechter parameters compared to the values determined previously in the literature up to z≈8. This plot indicates that α gets steeper towards higher redshift while M* becomes brighter out to z≈4. Furthermore, having fitted a function for α, M* and ϕ* as a function of z, it can be seen that our measured parameters especially the shallower alpha at z≈2 are in fact consistent with the overall redshift trend.

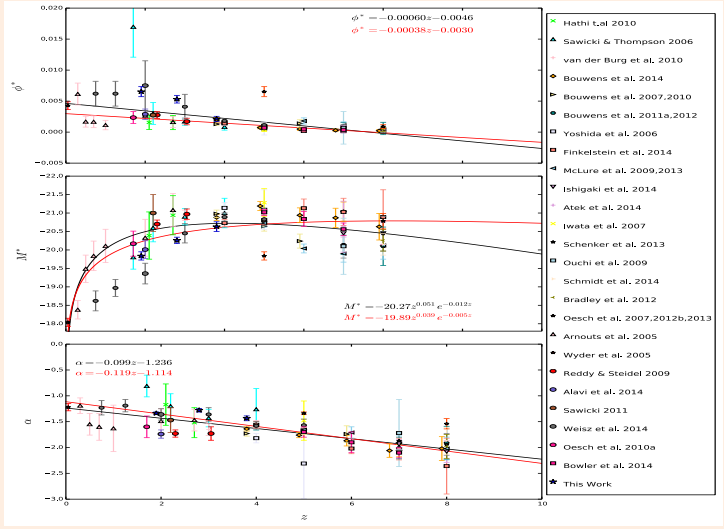

Figure 5. The evolution of the Schechter parameters with redshift. The filled stars show the measurements of this work. The black fitted line represents the evolution trend of these parameters as a function of z determined by considering only the data points; the parameter uncertainties have been considered in the red fitting.

Luminosity Density

Having derived a robust rest-frame UV LF at z≈2, 3 and 4, we can measure the observed luminosity densities at these epochs by integrating the luminosity-weighted LF. In this study three faint-end limits are considered: M_{1500}= -17.7, -15 and -10.

The results shown in Figure 6 imply that at all magnitude limits, the luminosity density and consequently the star formation rate peak at $2.5 < z < 3$.

To fairly compare our results to previous studies, we only consider the measured luminosity densities integrated down to M_{limit}= -17.7. This is shown in Figure 7.

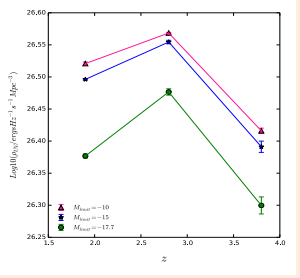

Figure 6. The rest-frame UV luminosity density integrated to M_{1500}= -10 (pink triangles), -15 (blues stars) and -17.7 (green circles). This plot indicates that the luminosity density and consequently the star formation rate peaks at z=2.5-3 .

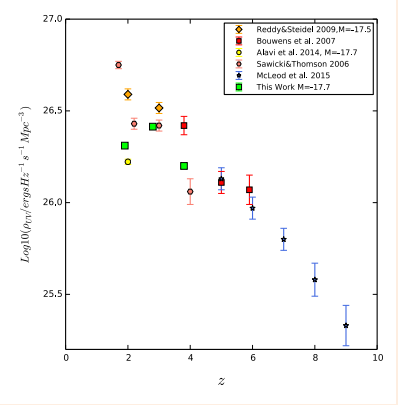

Figure 7. The rest-frame UV luminosity density at different epochs calculated in this work and previous studies.

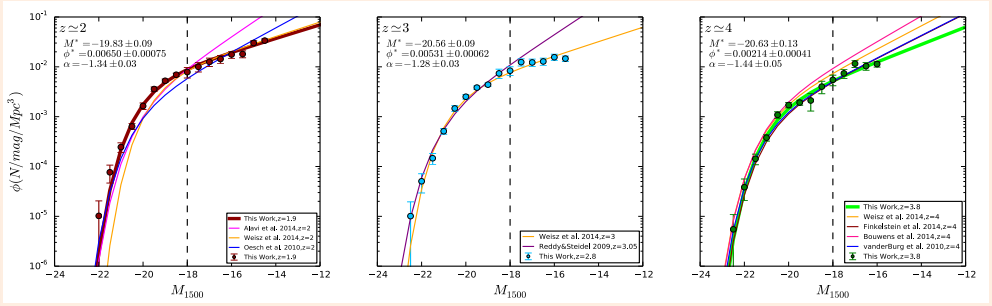

Figure 4. The rest-frame UV LFs at z≈2-4 with the best-fitting Schechter function. Dashed line at M=-18 represents the average faintest bin reached by other studies at these redshifts. At each epoch, several LFs from the literature are also shown and the corresponding studies are indicated in the legend.

Conclusion

The combination of wide area and deep CANDELS/GOODS-S survey with the extremely deep HUDF12 dataset has allowed us to determine the rest-frame UV LF down to M_{1500}= -14.5, -15.5 and -16 for z≈2,3,4 respectively. We find a substantially shallower α≈-1.34 at z≈2 than several previous studies but confirm little evolution in the LF from z=2 to 3.

Our results imply that the UV luminosity density peaks at z≈3 but is somewhat lower than previously determined due to our flatter faint end slope.

Ref :
Alavi A. et al., 2014, ApJ, 780
Ilbert O. et al., 2006, A&A, 457, 841
Oesch P. A. et al., 2010, ApJL, 725
Reddy N. A., Steidel C. C., 2009, ApJ, 692, 778
Sawicki M., Thompson D., 2006, ApJ, 642, 653
Weisz D. R.,Johnson B. D.,Conroy C., 2014, ApJL, 794